

Characterization of Hepatitis C Virus Recombinants with Chimeric E1/E2 Envelope Proteins and Identification of Single Amino Acids in the E2 Stem Region Important for Entry

Thomas H. R. Carlsen,^a Troels K. H. Scheel,^a Santseharay Ramirez,^a Steven K. H. Fong,^b Jens Bukh^a

Copenhagen Hepatitis C Program, Department of Infectious Diseases and Clinical Research Centre, Copenhagen University Hospital, Hvidovre, and Department of International Health, Immunology, and Microbiology, Faculty of Health Sciences, University of Copenhagen, Copenhagen, Denmark^a; Department of Pathology, Stanford University School of Medicine, Stanford, California, USA^b

The hepatitis C virus (HCV) envelope proteins E1 and E2 play a key role in host cell entry and represent important targets for vaccine and drug development. Here, we characterized HCV recombinants with chimeric E1/E2 complexes *in vitro*. Using genotype 1a/2a JFH1-based recombinants expressing 1a core-NS2, we exchanged E2 with functional isolate sequences of genotypes 1a (alternative isolate), 1b, and 2a. While the 1a-E2 exchange did not impact virus viability, the 2a-E2 recombinant was nonviable. After E2 exchange from three 1b isolates, long delays were observed before spread of infection. For recovered 1b-E2 recombinants, single E2 stem region amino acid changes were identified at residues 706, 707, and 710. In reverse genetic studies, these mutations increased infectivity titers by ~100-fold, apparently without influencing particle stability or cell binding although introducing slight decrease in particle density. In addition, the 1b-E2 exchange led to a decrease in secreted core protein of 25 to 50%, which was further reduced by the E2 stem region mutations. These findings indicated that compensatory mutations permitted robust infectious virus production, without increasing assembly/release. Studies of E1/E2 heterodimerization showed no differences in intracellular E1/E2 interaction for chimeric constructs with or without E2 stem region mutations. Interestingly, the E2 stem region mutations allowed efficient entry, which was verified in 1a-E1/1b-E2 HCV pseudoparticle assays. A CD81 inhibition assay indicated that the mutations influenced a late step of the HCV entry pathway. Overall, this study identified specific amino acids in the E2 stem region of importance for HCV entry and for production of infectious virus particles.

Hepatitis C virus (HCV) is a major public health burden, with 130 to 170 million people persistently infected worldwide (1). There is no vaccine available. The current treatment combining pegylated alpha interferon and ribavirin was recently supplemented with directly acting protease inhibitors (2). For regimens based on alpha interferon and ribavirin, for which most knowledge is available, cure rates are around 50% and depend on the viral genotype, with genotype 1 being the least sensitive. However, treatment is associated with severe side effects (3), and the use of novel directly acting antivirals is challenged by viral escape mutants. Thus, to improve the development of an HCV vaccine and more efficient treatment regimens, it is important to gain additional knowledge about the HCV life cycle and thereby identify essential components of the HCV genome and expressed proteins. The envelope proteins, and in particular specific residues with key impact on entry and/or glycoprotein functionality, could potentially constitute a valuable treatment target for HCV, e.g., through development of entry inhibitors and neutralizing antibodies, and could be of great importance for development of a prophylactic vaccine (4–6). Numerous drugs and antibodies targeting the entry step have been developed and analyzed (7–13). None of these therapeutic interventions have so far reached the clinic, and a better characterization of E1 and E2 is important to improve targeting of these proteins. In this study, viruses with chimeric HCV envelope proteins were studied with the aim to identify specific regions and residues critical for HCV viability.

HCV is a small, enveloped, single-strand RNA virus belonging to the *Flaviviridae* family. The HCV genome is 9.6 kb in length and consists of a 5′ untranslated region (UTR), an open reading frame (ORF), and a 3′ UTR. The ORF encodes a single polyprotein,

which is co- and posttranslationally cleaved into the structural proteins (core, E1, and E2), p7, and the nonstructural (NS) proteins (NS2, NS3, NS4A, NS4B, NS5A, and NS5B) (14). HCV strains are genetically diverse, and have been grouped into seven major genotypes and multiple subtypes. Nucleotide sequence variability between genotypes is around 30%; between subtypes, it is 20 to 25%. Furthermore, genetic diversity between isolates belonging to the same subtype is on average 5%, with the envelope proteins exhibiting high genetic heterogeneity (15–18).

During HCV polyprotein processing, E1 and E2 are released by host signal peptidases (19). Both proteins are heavily glycosylated on the N-terminal ectodomain in the lumen of the endoplasmic reticulum (ER) (20). The C-terminal ends of E1 and E2 contain transmembrane (TM) domains, which are inserted into the intracellular lipid membrane of the ER (21). During particle assembly, E1 and E2 interact noncovalently and form a heterodimer on the surface of the viral particle. Disulfide bridges stabilize the heterodimer as the complete virion is released from the host cell (22). Previous studies have shown that the C-terminal TM domains are important during E1/E2 heterodimerization (23) and that a part

Received 18 March 2012 Accepted 30 October 2012

Published ahead of print 14 November 2012

Address correspondence to Jens Bukh, jbukh@sund.ku.dk.

Supplemental material for this article may be found at <http://dx.doi.org/10.1128/JVI.00684-12>.

Copyright © 2013, American Society for Microbiology. All Rights Reserved.

doi:10.1128/JVI.00684-12

of the E2 ectodomain is involved in this dimerization (24). Furthermore, the E1/E2 dimer and specific domains within this complex, including the E2 stem region connecting the TM domain with the ectodomain, influence viral entry (22, 24, 25).

Studies of the HCV envelope proteins and entry were initially facilitated by development of the HCV pseudoparticle (HCVpp) system (26, 27). Subsequent establishment of complete HCV cell culture systems (HCVcc) allowing studies of all steps of the viral life cycle led to great advances in basic studies of HCV (28, 29). Furthermore, JFH1-based intra- and intergenotypic cell culture systems enabled genotype-, subtype-, and isolate-specific studies on the HCV structural proteins, p7, and NS2 (28, 30–33). In this study, we aimed at further characterizing the HCV envelope proteins with the intention to reveal domains and residues important for virus viability. Through exchange of the E2 gene from a JFH1-based recombinant expressing core-NS2 from genotype 1a isolate H77C with corresponding functional E2 sequences from different genotype 1a, 1b, and 2a isolates, we identified single compensatory mutations in a 5-amino-acid (aa) stretch of the E2 stem region and characterized their importance for the HCV life cycle. Our study provides novel insight into the compatibilities between the HCV envelope proteins and analyzes the impact of specific residues in the E2 stem region on the functionality of HCV particles.

MATERIALS AND METHODS

Plasmids and construction of E2 exchange recombinants. We used the previously developed cell culture-adapted JFH1-based intergenotypic 1a/2a recombinants pH77C/JFH1_{V787A Q1247L} and pH77C/JFH1_{Q1247L} (33) as backbones and exchanged the E2 gene. The inserted E2 genes were from molecular clones of one 1a isolate (TN) (34), three 1b isolates (J4, DH1, and DH5) (31, 32), and one 2a isolate (J6) (35), all of which had previously been verified to be functional. The exchange of the E2 gene was done using standard fusion PCR and cloning procedures. Introduction of putative compensatory mutations was performed using site-directed mutagenesis, and the HCV sequences of the final plasmid preparations were confirmed.

As a positive control, we included the previously developed JFH1-based recombinant pH77C/JFH1_{V787A Q1247L} (33). As negative controls, we used the nonadapted pH77C/JFH1, which was previously shown to be defective in assembly (32), pJFH1_{ΔE1/E2} (29), which lacks most of the E1/E2 genes and therefore does not produce virus, and the replication-deficient 1b/2a recombinant pDH5/JFH1_{4aa} containing a 4-amino-acid insertion at the NS2/NS3 junction. The replication-deficient recombinant pJ6/JFH1-GND (28) was included in relevant assays.

Huh7.5 and S29 cell culture assays. *In vitro* transcription, transfection, and culturing of Huh7.5 hepatoma cells (28) and S29 CD81-deficient hepatoma cells (36) and infection of Huh7.5 cells were performed as previously described (30, 33). Cells were in complete medium prior to transfection with Lipofectamine 2000 (Invitrogen). In relevant assays, medium was replaced with Opti-MEM (Invitrogen) before transfection to increase transfection efficiency (37). Opti-MEM or complete medium containing Lipofectamine 2000 was replaced with complete medium at 4 h or 16 h posttransfection. Spread of infection was analyzed by immunostaining against the NS5A protein using anti-NS5A antibody (9E10 [28]) as previously described (30, 33).

For determination of infectivity titers, 6×10^3 cells/well were plated in poly-D-lysine-coated 96-well plates (Nunc) at 24 h before infection with appropriate virus dilutions (minimum, 1:2) in triplicates and were incubated for an additional 48 h before fixation and immunostaining following a previously developed protocol (30). Focus-forming units (FFU) were determined by automatic quantification using an ImmunoSpot series 5 UV analyzer (CTL Europe, GmbH), as previously described (38). In this assay, the background was defined as the mean FFU count of 6 nega-

tive wells, which was subtracted from each FFU count in positive wells. The lower limit of quantification was set to the background value plus 3 standard deviations plus 3. This value allowed counting of titers of $>10^{2.3}$ FFU/ml. Cultures with infectivity titers below the detection limit were in selected experiments counted manually using a light microscope, lowering the detection limit of the titration to $10^{1.3}$ FFU/ml and $10^{0.7}$ FFU/well for extracellular and intracellular titers, respectively. In manual counting, a minimum of 1 FFU/well in all triplicate wells was set as the lower limit of a positive sample. For quantification of intracellular infectivity titers, 4×10^5 S29 cells were transfected with *in vitro*-transcribed HCV RNA. Transfected S29 cells were harvested at 48 h posttransfection, resuspended in 100 μ l complete medium, and freeze-thaw lysed in liquid nitrogen and a 37°C water bath in four repeated cycles for the release of HCV particles. Cell debris was removed from the suspension by two centrifugations at $1,500 \times g$ at 4°C for 15 min prior to titration on Huh7.5 cells as stated above (minimum dilution, 1:5).

HCV core antigen ELISA. For measurements of intra- and extracellular HCV core concentrations, we used the Ortho HCV antigen enzyme-linked immunosorbent assay (ELISA) kit (Ortho Clinical Diagnostics) in accordance with the manufacturer's protocol. For quantification of intracellular core concentration, 4×10^5 S29 cells seeded the day before in 6-well plates were transfected with HCV RNA transcripts in Opti-MEM as described above. Cells were harvested at 4 h and 48 h posttransfection, and one-fourth of the harvested cells were centrifuged at $1,000 \times g$ for 5 min at 4°C. Following a wash in cold sterile phosphate-buffered saline (PBS), the cell pellet was lysed in 100 μ l radioimmunoprecipitation assay (RIPA) buffer (Thermo Scientific) containing protease inhibitor cocktail set III (Calbiochem) (32). For extracellular quantification of core concentration, sterile filtered supernatant was analyzed directly at appropriate dilutions.

Equilibrium density gradient analysis. For equilibrium density analysis, around 8 ml of virus supernatant was concentrated to $\sim 250 \mu$ l using Amicon centrifugation filters (Millipore) prior to loading onto semicontinuous gradients. Gradients were created by applying layers of 40%, 30%, 20%, and 10% OptiPrep (iodixanol; Axis-Shield) in sterile PBS in steps of 2.5 ml to ultracentrifugation tubes (Beckman). The layers were added gently sequentially and left at 4°C overnight for gradient formation. Equilibrium was obtained through ultracentrifugation at 35,000 rpm for 18 h at 4°C using a swinging-bucket Beckman SW-41 rotor in a Beckman XL-70 ultracentrifuge. Following centrifugation, 15 fractions of $\sim 700 \mu$ l were harvested from bottom to top, and densities were calculated. Each fraction was analyzed for infectivity titers (minimum dilution, 1:10) and core concentration as described above. The titration detection limit of the manual counting in this assay was $10^{2.0}$ FFU/ml.

HCV particle thermostability assay. Virus supernatants from S29 transfected cells were harvested at 48 h posttransfection. The harvested supernatants were aliquoted in volumes of 320 μ l and incubated at 37°C for 0 h, 4 h, 8 h, 16 h, 24 h, and 32 h. At each time point, an aliquot was transferred to -80°C for later virus titration. Aliquots from each time point were incubated with naïve Huh7.5 cells and titrated in triplicates as described above.

HCV particle binding assay. Huh7.5 cells (4×10^5 cells/well) were plated in 6-well plates (Nunc) 1 day prior to the particle binding assay. For the assay, naïve Huh7.5 cells were incubated on ice for 5 min, and 4 ml of S29 cell-produced supernatant was applied to cells and incubated at 4°C for 2 h to obtain particle binding to cells. Cells were washed twice in 4°C PBS, lysed directly in 150 μ l RIPA buffer (Thermo Scientific) containing protease inhibitor cocktail set III (Calbiochem), and transferred to ice for 15 min with frequent agitation. Cell lysates were centrifuged at $20,000 \times g$ for 20 min at 4°C and subjected to core ELISA as described above.

CD81 receptor-blocking assay. We previously described the CD81 antibody-blocking assay (30). In short, 6×10^3 Huh7.5 cells/well were plated in poly-D-lysine-coated 96-well plates (Nunc). After 24 h, cells were incubated with anti-CD81 (JS-81; BD Biosciences) or an isotype-matched control antibody (BD Biosciences) for 1 h, followed by addition of S29

cell-produced HCVcc. After 48 h, the number of FFU in each well was determined as described above.

HCVpp assays. Huh7.5 cells and human embryo kidney (HEK) 293T cells were cultured at 37°C with 5% CO₂ in Dulbecco modified Eagle medium (DMEM) supplemented with 10% fetal bovine serum (FBS) and antibiotics (Invitrogen). The plasmids used to generate HCV pseudoparticles (HCVpp) were murine leukemia virus (MLV) Gag-Pol, MLV-luc, and phCMV-ires, provided by François-Loïc Cosset (39, 40). For generation of HCV expression plasmids, the sequence encoding the last 60 amino acids of core and the entire E1 and E2 genes were amplified by PCR from the HCVcc recombinant plasmids J4/JFH1, DH1/JFH1, and DH5/JFH1 (31, 32) using strain-specific primers. The reverse primer contained a stop codon, which was introduced after the last amino acid of E2, and amplicons were cloned into the phCMV-ires vector using the EcoRV restriction site. The sequence of the HCV insert was confirmed for the final preparation of all constructed plasmids.

To generate each batch of HCVpp, 2.5×10^6 HEK 293T cells were seeded in 10-cm dishes (Nunc) at 24 h prior to transfection. Transfection was performed with 8 µg of Gag-Pol, 8 µg of MLV-luc, and 4 µg of HCV envelope plasmids using a commercially available calcium phosphate protocol (Clontech Laboratories Inc.) and following the manufacturer's instructions. Medium was replaced at 6 h posttransfection, and cells were kept in culture for 48 h. Supernatants containing HCVpp were collected and filtered through 0.45-µm-pore-size membranes, and one aliquot was used directly for the infection assays whereas another aliquot was stored at -80°C for further analysis of HCVpp. In addition, the transfected cells were lysed in RIPA buffer (Thermo Scientific) and stored at -80°C for further analysis.

For infection assays, 1.5×10^4 Huh7.5 cells/well were seeded in 96-well plates (96-well optical-bottom plates; Nunc) at 24 h prior to infection with fresh collected supernatants. A final volume of 100 µl containing the supernatants and Polybrene at a final concentration of 4 µg/ml was added to the cells, and infection was continued for 12 h. Afterwards, the infection mixture was replaced by 200 µl of fresh medium, and cells were incubated for an additional 72 h. For analysis, cells were washed with PBS, followed by lysis with luciferase cell culture lysis reagent (Promega) for 10 min. Luciferase measurements were performed with a FluoStarOptima microplate reader (BMG; Labtech) after addition of firefly luciferase substrate (luciferase assay system; Promega). Background values measured in non-infected cells were subtracted from luminescence measurements. The statistical significance of the infectivity differences was tested with the Wilcoxon rank sum test.

Co-IP assay. 293T cells (3×10^6 /well) were seeded in 10-cm dishes. After 24 h, cells were transfected with phCMV-ires vectors expressing the last 60 amino acids of core and the entire E1 from H77 and E2 from H77, J4, DH1, or DH5, as described above. Transfection was performed with 20 µg of HCV envelope plasmids using the calcium phosphate protocol as described above. Medium was replaced at 6 h posttransfection, and cells were kept in culture for 24 h. Coimmunoprecipitation (co-IP) was conducted with the Dynabeads coimmunoprecipitation kit (Invitrogen) following the manufacturer's guidelines. One day prior to co-IP, beads were coated with either glutathione S-transferase (GST)-tagged CD81 large extracellular loop (CD81-LEL-GST) (41) or GST tag (Novus Biologicals) using 20 µg protein/1.5 mg beads. Approximately 0.05 g of transfected 293T cells was lysed, and co-IP was performed using either CD81-LEL-GST- or GST-coated beads, followed by immunoblot detection (as described below) of E1 and E2 in the elution fractions and of E1, E2, and β-actin in the input lysate.

Concentration of HCVcc and HCVpp using ultracentrifugation. Concentration of HCVcc and HCVpp from collected supernatants was conducted using a cushion consisting of 2 ml 20% sucrose (Sigma) in sterile PBS. Supernatant was layered on top of the cushion and subjected to ultracentrifugation at 25,000 rpm for 3 h at 4°C using a centrifuge and rotor as described above. The pelleted particles were dissolved in either 60

µl or 100 µl sterile PBS and stored overnight at 4°C or for longer terms at -80°C before use in Western blot analysis.

WB. Western blotting (WB) analysis was performed on ultracentrifuged HCVcc, HCVpp, or transfected HEK293T cells. Prior to immunoblotting, transfected HEK293T cells were lysed in four freeze-thaw cycles as stated above for S29 cells and clarified by centrifugation at 14,000 rpm for 15 min. Proteins were denatured at 70°C for 10 min in the presence of NuPAGE sample reducing agent (Invitrogen) and NuPAGE LDS sample loading buffer (Invitrogen). Proteins were separated through a 12% bis-Tris SDS-polyacrylamide gel (Invitrogen) and subsequently transferred to a 0.45-µm Hybond-P polyvinylidene difluoride (PVDF) membrane (GE Healthcare Amersham) by using a XCell SureLock minicell (Invitrogen).

Membranes were incubated overnight at 4°C with specific antibodies, i.e., anti-core (C7-50 [Enzo Life Science]), anti-E1 (A4 [42]), anti-E2 (H52 [42]), anti-Gag-MLV (25), or anti-β-actin (Santa Cruz Biotechnologies), followed by 1 h of incubation with ECL sheep anti-mouse IgG horseradish peroxidase-linked whole antibody (GE Healthcare Amersham). Target proteins were visualized using Signal West Femto maximum-sensitivity substrate (Pierce) and AutoChemi Systems (UVP Bio-Imaging Systems) for chemiluminescence detection.

Sequence analysis. RNA extraction from cell culture supernatant followed by reverse transcription and amplification for direct sequencing was performed as previously described (30, 32, 33). Sequence analysis of amplicons (sequenced directly) and final plasmid preparations were performed with Sequencher (Gene Codes). Initially, the complete ORF of each of the E2 exchange recombinants from the recovered viruses was sequenced. However, as only one partial mutation in NS4B and a few sporadic mutations in NS5A were identified, the remaining recovered viruses were sequenced only from core-NS2 (see Table S1 in the supplemental material). Multiple-sequence alignment analysis was done using Molecular Evolutionary Genetics Analysis 4 (MEGA4) (43). The design of cloning strategies for E2 exchange recombinants was carried out with Vector NTI Advanced 11 (Invitrogen). HCV sequences for multiple alignments were downloaded from the Los Alamos hepatitis C sequence database (44).

RESULTS

Effect on virus viability of exchange of the HCV E2 protein between isolates, subtypes, and genotypes. To further our understanding of the role of E1 and E2 glycoproteins in the context of the complete HCV life cycle, we here aimed at identifying and characterizing specific residues of importance for a functional E1/E2 complex. We initially exchanged the E2 gene of a previously developed genotype 1a/2a JFH1-based intergenotypic core-NS2 recombinant (strain H77C) with corresponding functional sequences from a different genotype 1a isolate, three genotype 1b isolates, and one genotype 2a isolate. By transfecting RNA transcripts from the E2-exchanged recombinants into Huh7.5 hepatoma cells, we aimed at determining whether the H77C (1a) core, E1, p7, and NS2 proteins would be compatible with E2 proteins of different isolates, subtypes, and genotypes.

For the H77C/JFH1_{Q1247L}(TN-E2) recombinant, which carried the E2 gene from another genotype 1a isolate, infectivity titers and spread of infection (immunostaining against the NS5A protein) after transfection were comparable to what was previously reported for the H77C/JFH1_{Q1247L} recombinant (33) (Fig. 1). Peak infectivity titers were $10^{4.0}$ FFU/ml on day 4 posttransfection, and we did not observe requirements for mutations in sequence analysis of supernatant viruses recovered 11 days after cell-free passage to naïve Huh7.5 cells. In contrast, we observed an eclipse phase of 32 days before spread of infection to ~60% of cells for the H77C/JFH1_{Q1247L}(J4-E2) recombinant, in which the E2 gene was from a genotype 1b isolate. The peak titer observed for J4-E2 was

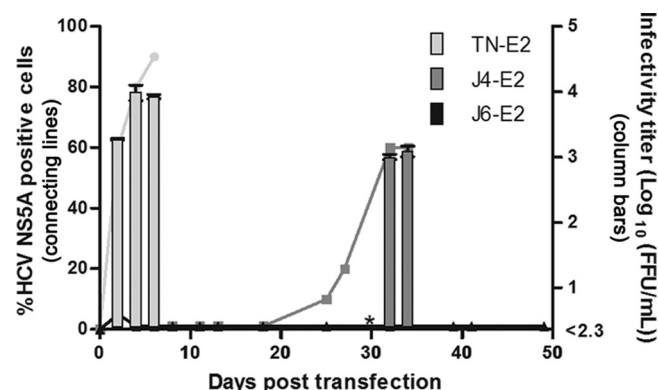


FIG 1 Viability of E2-exchanged HCV recombinants. *In vitro*-generated RNA transcripts of H77C/JFH1_{Q1247L} (TN-E2), H77C/JFH1_{Q1247L} (J4-E2), and H77C/JFH1_{Q1247L} (J6-E2) recombinants were transfected into Huh7.5 cells. The connecting lines represent the percent HCV NS5A-positive cells as determined by immunostaining at the indicated time points posttransfection (left y axis). The column bars show the infectivity titers for the E2-exchanged recombinants, which spread in culture following transfection (right y axis). Titer values are means of triplicates, with error bars displaying standard errors of the means (SEM). The lower limit of quantification was $10^{2.3}$ FFU/ml. *, measured virus supernatant under the limit of quantification.

$10^{3.1}$ FFU/ml on day 32 posttransfection. Direct sequence analysis of HCV recovered from supernatant at this time point identified only one amino acid change, V710F (Table 1; see also Table S1 in the supplemental material) (numbering throughout is according to the H77 reference sequence, GenBank accession number AF009606). Finally, in 2 replicate transfections of the H77C/JFH1_{Q1247L} (J6-E2) recombinant, in which the E2 gene was from a genotype 2a isolate, positive cells could be detected until day 49 but with no evidence of viral spread. The cultures were thereafter negative until day 67 (end of follow-up). Thus, we found that exchanging E2 with an isolate of the same subtype was permissible and that our method allowed studies of possible incompatibilities with E2 from another subtype of genotype 1.

To achieve a better understanding of cross-subtype incompatibilities for E2, we performed a total of five replicate transfections in Huh7.5 cells with each of the 1b-E2-exchanged recombinants J4-E2, DH1-E2, and DH5-E2. All recombinants spread to infect the majority of the cells after an eclipse phase of 27 to 34 days, while H77C/JFH1_{V787A Q1247L} infected $>80\%$ of cells no later than day 8. In contrast, no infected cells were observed at any time point for the replication-deficient JFH1-based core-NS2 recombinant, DH5/JFH1_{4aa}, containing a 4-amino-acid insertion in the NS2/NS3 junction. Supernatants collected at peak infection time points (i.e., $\geq 80\%$ positive infected cells) were analyzed further. Core-NS2 sequence analysis of recovered viruses from the five independent transfections revealed that all recombinants had acquired mutations in at least one of the envelope genes (Table 1). Interestingly, 9 of 15 transfections contained mutations (either complete amino acid changes or a mixture of the original and the mutant sequences) within a five-amino-acid stretch, from aa 706 to 710, in the stem region of E2. Changes at specific residues were associated with each of the three 1b-E2 recombinants (Table 1). We found mutations at amino acid position 710 (V to F or V to G) in 3 of 5 transfections for J4-E2. Furthermore, changes at aa 706 (G to R) were observed in 4 of 5 transfections for DH1-E2, and a change at position 707 (S to L) was observed in 2 of 5 transfections

for DH5-E2. The aa 706 change (G to R) was also seen in one of these DH5-E2 transfections.

Single mutations in the E2 stem region fully restore virus viability of E2-exchanged recombinants. We performed reverse genetic studies by introducing the identified single putative compensatory mutations into the respective recombinants to investigate their influence on virus viability. After transfection into Huh7.5 cells, infection spread and infectivity titers for J4-E2_{V710F}, DH1-E2_{G706R}, and DH5-E2_{S707L} recombinants were comparable to those for H77C/JFH1_{V787A Q1247L} (Fig. 2A to C). Peak infectivity titers for the mutated 1b-E2 recombinants ranged from $10^{4.0}$ to $10^{4.4}$ FFU/ml within 6 to 10 days posttransfection. In contrast, each of the original E2-exchanged isolates without putative compensatory mutations produced viral titers of $\sim 10^{2.0}$ FFU/ml (Fig. 2A to C). Finally, the J4-E2_{V710F}, DH1-E2_{G706R}, and DH5-E2_{S707L} recombinants did not acquire mutations in core-NS2 after passage to naïve Huh7.5 cells (see Table S1 in the supplemental material).

Next, we tested whether the E2 stem region mutations, which restored infectivity for the 1b-E2 recombinants from which they had been recovered, also would restore infectivity for the other 1b-E2 recombinants. We thus introduced G706R or S707L into J4-E2, S707L or V710F into DH1-E2, and G706R or V710F into DH5-E2 and tested viability by transfection of Huh7.5 cells (Fig. 2D). All mutants exhibited accelerated growth kinetics, as defined by viral spread, compared to the original E2-exchanged recombinants. However, the J4-E2 and DH1-E2 mutants depended on additional mutations, including mutations in the E2 stem region, for efficient production of infectious viral particles (see Table S1 in the supplemental material). In contrast, DH5-E2_{G706R} and DH5-E2_{V710F} did not acquire further mutations after passage to naïve Huh7.5 cells. For these DH5-E2 recombinants, we observed peak infectivity titers of $10^{4.2}$ and $10^{3.6}$ FFU/ml at days 6 and 8 posttransfection, respectively (Fig. 2D).

Thus, introduction of single E2 stem region mutations, identified from recovered genotype 1b-E2-exchanged recombinants, led to efficient spread in cell culture and production of peak infectivity titers comparable to those for H77C/JFH1_{V787A Q1247L} when introduced into recombinants of the same E2 isolate. Introduction of the mutations into other 1b-E2 isolates accelerated growth kinetics, although additional mutations were required for most recombinants to efficiently infect the cell culture. Overall, these results provided evidence for an isolate-specific interaction between aa 706 and 710 in the stem region of E2 and core, E1, p7, or NS2, since the inserted E2 isolates are known to be compatible with the JFH1 NS3-NS5B proteins (31, 32).

E1 and E2 mutations identified outside the E2 stem region influence virus viability of 1b-E2 recombinants. To analyze the importance of mutations outside the E2 stem region in 1b-E2 recombinants without stem region mutations, we selected specific mutations identified in transfections for each of the three E2-exchanged recombinants (Table 1). For J4-E2, the E1 mutation I262F and the E2 mutation T475A (identified in the third transfection) were introduced alone and in combination. The E1 mutation M324T (identified in the fifth transfection) was introduced into the DH1-E2 recombinant, while the E2 mutations V414A and L725F (identified in the first transfection) were introduced alone or combined into DH5-E2. Prior to testing, the persistence of the mutations selected for further analysis was confirmed in cell-free passage to naïve cells. Following transfection into Huh7.5 cells, 5 of 7 developed recombinants spread to the majority of cells within

TABLE 1 E1 and E2 mutations identified from H77(core-NS2)/FH1 recombinant with E2 from 1b strains J4, DH1, and DH5 following transfection of Huh7.5 cells^a

Sequence type, recombinant, and transfection no.		Day post- trans- fection	Nucleotide or amino acid change at the indicated position ^b																			
			E1 gene										E2 gene									
Nucleotide number	1013	1121	1124	1124	1311	1329	1344	1347	1581	1590	DII (aa 445-521)		DIb (aa 522-580)		DIII (aa 581-650)		Stem region (aa 651-715)		TM (aa 716-746)			
pJ4-E2	G	C	A	A	T	C	C	A	T	A	A	A	A	A	A	C	A	G	C	G	T	
1 ^c	32	
2 ^c	45	
3 ^d	27	.	.	T	G	.	.	A/G	
4 ^d	36	.	C/T	A/G	
5 ^d	34	
PDH1-E2	G	C	A	A	T	C	C	A	T	A	A	G	A	A	A	C	A	G	C	G	T	
1 ^c	27	A	.	.	.	
2 ^c	27	C/A	A/g	.	.	.	
3 ^d	34	T/C	C/a	G/C	.	.	.	
4 ^d	27	C	.	C/a	G/a	.	.	.	
5 ^d	27	
PDH5-E2	G	C	A	A	T	C	C	A	T	A	A	A	A	A	A	T	A	G	C	G	T	
1 ^c	29	
2 ^d	34	G/A	C/T	.	.	
3 ^d	31	G/T	C/A	.	T/C	.	.	.	A/G	
4 ^d	34	T/C	
5 ^d	34	.	.	.	A/G	C	A	.	.	C/T	.	T	
Amino acid position	225	261	262	262	324	329	335	336	414	417	474	475	532	578	586	595	706	707	710	710	714	
Change	G→W	Y→H	I→F	I→V	M→T	A→E	A→D	A→D	V→A	N→T	Y→C	T→A	N→S	T→A	F→L	T→A	G→R	S→L	V→F	V→G	I→F	
																					L→F	
																					L→P	

^a All mutations identified from either full ORF or core-NS2 sequence analysis can be found in Table S1 in the supplemental material.^b Coding mutations in E1 and E2 are shown. At positions where a mutation was not dominant among the quasispecies, both nucleotides are stated, with the dominant one in capital letters. For a 50/50 population, both nucleotides are written in capital letters. DIIa, domain Ia; DIb, domain Ib; DII, domain II; DIII, domain III; TM, transmembrane domain. Mutation numbering is according to the H77 reference sequence (GenBank accession number AF009606).^c The complete ORF sequence was analyzed.^d The core-NS2 sequence was analyzed.

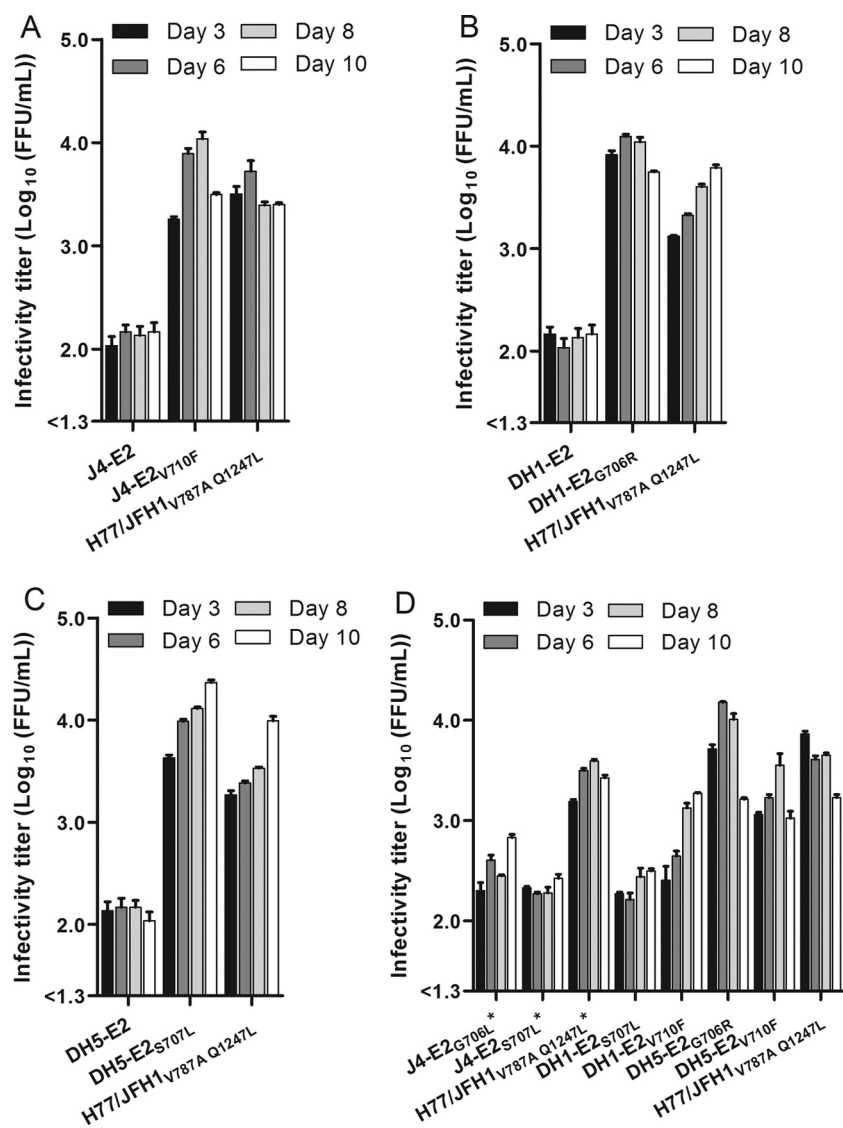


FIG 2 HCV infectivity titers after transfection of the 1b-E2 H77C/JFH1_{V787A Q1247L} recombinants with and without E2 stem region mutations. *In vitro*-generated RNA transcripts of H77C/JFH1_{V787A Q1247L} (J4-E2) with or without V710F (A), H77C/JFH1_{V787A Q1247L} (DH1-E2) with or without G706R (B), H77C/JFH1_{V787A Q1247L} (DH5-E2) with or without S707L (C), and H77C/JFH1_{V787A Q1247L} (J4-E2) with G706R or S707L, H77C/JFH1_{V787A Q1247L} (DH1-E2) with S707L or V710F, and H77C/JFH1_{V787A Q1247L} (DH5-E2) with G706R or V710F (D) were transfected into Huh7.5 cells. Virus production in the supernatant was measured on days 3, 6, 8, and 10 posttransfection. The previously developed H77C/JFH1_{V787A Q1247L} recombinant was included as a positive control. Amino acid residues were numbered according to the polyprotein of the H77 reference sequence (GenBank accession number [AF009606](#)). All titer values are means of triplicates, with error bars displaying standard errors of the means (SEM). The lower limit of quantification was 10^{1.3} FFU/ml. *, samples analyzed in a separate experiment.

10 days posttransfection. Peak infectivity titers of the viable recombinants ranged from 10^{3.5} to 10^{4.3} FFU/ml, which were comparable to the titers obtained for the H77C/JFH1_{V787A Q1247L} control (Fig. 3). Direct sequencing of first-passage day 16 J4-E2_{I262F}, DH1-E2_{M324T}, and DH5-E2_{V414A L725F} supernatant viruses revealed no need for further mutations. In contrast, we identified additional mutations in J4-E2_{I262F T475A} and in DH5-E2_{V414A} (see Table S1 in the supplemental material). Finally, J4-E2_{T475A} and DH5-E2_{L725F} were both attenuated and did not spread in culture within the analyzed time period.

Thus, for the majority of E2-exchanged recombinants, introduction of identified mutations outside the stem region influenced virus viability similarly to the stem region mutations. Fur-

ther, for two E2 recombinants, J4-E2 and DH1-E2, introduction of single E1 mutations led to fully viable virus, indicating that the compensatory mutation in genotype 1a E1 was enough to ensure proper interaction with the chimeric 1b E2 protein.

Compensatory mutations in the stem region of E2 do not influence HCV replication. To investigate the functional role of the E2 stem region, in which compensatory mutations were identified for all E2-exchanged recombinants, we next analyzed the mutants in assays that addressed different steps of the viral life cycle. To determine if HCV replication capacity was affected by the mutations, we quantified intracellular HCV core levels after transfection of CD81-deficient hepatoma cells (S29 cells) (36), which allows single-cycle studies as they are nonpermissible to

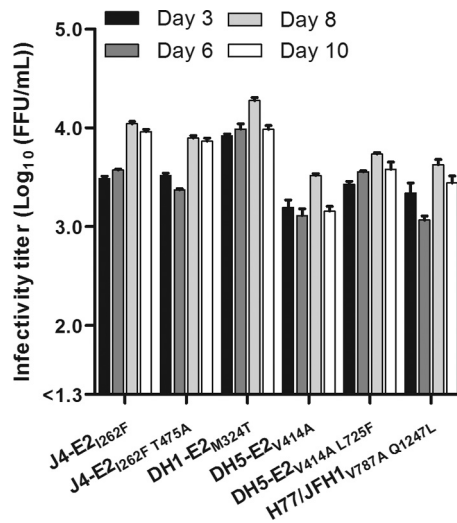


FIG 3 HCV infectivity titers after transfection of the 1b-E2 H77C/JFH1_{V787A Q1247L} recombinants containing mutations identified outside the E2 stem region. *In vitro*-generated RNA transcripts of J4-E2_{I262F}, J4-E2_{I262F} T475A, DH1-E2_{M324T}, DH5-E2_{V414A}, and DH5-E2_{V414A L725F} (see Table S1 in the supplemental material) were transfected into Huh7.5 cells. Virus production in the supernatant was measured on days 3, 6, 8, and 10 posttransfection. The previously developed H77C/JFH1_{V787A Q1247L} recombinant was included as positive control. Amino acid residues were numbered according to the polypeptide of the H77 reference sequence (GenBank accession number AF009606). All titer values are means of triplicates, with error bars displaying standard errors of the means (SEM). The lower limit of quantification was 10^{1.3} FFU/ml.

HCV entry. We did not observe significant differences in the intracellular core levels between the E2-exchanged recombinants with or without E2 stem region mutations (Fig. 4). In addition, replication of the 1b-E2 H77C/JFH1_{V787A Q1247L} recombinants was comparable to that of H77C/JFH1_{V787A Q1247L}. These results confirmed that HCV replication was not influenced by the E2 gene exchange or by the acquisition of compensatory E2 stem region mutations.

Influence of E2 exchange and stem region mutations on HCV assembly/release. We further analyzed potential effects of the introduced compensatory E2 stem region mutations on assembly and release of viral particles. S29 cells transfected with RNA transcripts from the E2-exchanged recombinants with or without compensatory mutations were harvested at 48 h posttransfection, and intracellular particles were released through repeated freeze-thaw cycles. Intra- as well as extracellular titers for all 1b-E2 recombinants harboring E2 stem region mutations were higher than or comparable to those for H77C/JFH1_{V787A Q1247L}. Intracellular infectivity titers were in the range from 10^{3.1} to 10^{3.5} FFU/well (Fig. 5A), and extracellular titers ranged from 10^{3.7} to 10^{4.2} FFU/ml (Fig. 5B). In contrast, the original E2-exchanged recombinants had smaller amounts of intra- and extracellular infectious virus, with titers from 10^{2.2} to 10^{2.4} FFU/well and from 10^{2.3} to 10^{2.4} FFU/ml, respectively. Thus, the production of intra- and extracellular infectious particles was decreased for E2-exchanged recombinants without mutations, which was not caused by defects in virus release.

To assess whether similar amounts of total core protein were released for the original 1b-E2 recombinants and the corresponding recombinants with E2 stem region mutations, we performed

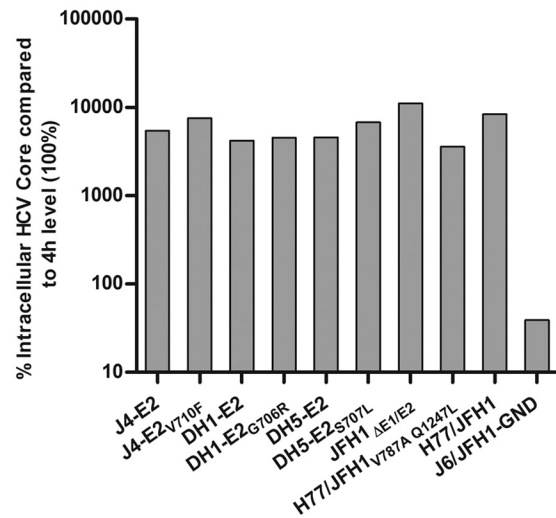


FIG 4 Determination of intracellular core concentration at 4 h and 48 h posttransfection of transfected S29 cells, as a measure for HCV replication. Intracellular core protein synthesis was quantified using HCV core antigen ELISA on lysed S29 cells transfected with RNA transcripts of 1b-E2 H77C/JFH1_{V787A Q1247L} recombinants with or without compensatory E2 mutations. For each recombinant, the core level measured at 48 h posttransfection is shown as a percentage of the 4-h core level (100%) in one replicate. Controls were H77C/JFH1_{V787A Q1247L} (positive control), H77C/JFH1 (assembly defective), JFH1_{ΔE1/E2} (lacking expression of envelope proteins), and J6/JFH1-GND (replication defective).

core antigen ELISA on supernatants from transfected S29 cells collected at 48 h posttransfection. The extracellular concentration of core protein was significantly lower for the original J4-E2 ($P = 0.04$), DH1-E2 ($P = 0.01$), and DH5-E2 ($P = 0.04$) than for H77C/JFH1_{V787A Q1247L} (Fig. 6A), suggesting an attenuated assembly/release following exchange of the E2 gene. The presence of compensatory E2 mutations further decreased the extracellular core levels for all E2-exchanged recombinants in three separate assays ($P = 0.02$), conferring on these a higher specific infectivity. This suggests that these mutations did not restore virus assembly but influenced another step of the HCV life cycle. Interestingly, the attenuation observed for the original 1b-E2 H77C/JFH1_{V787A Q1247L} recombinants was different from that for JFH1_{ΔE1/E2} and the nonadapted H77C/JFH1, which did not produce any extracellular core and were attenuated at the assembly step (Fig. 6A and previous results for H77C/JFH1 [32]). Thus, these mutations apparently led to a decrease in secretion of particles, which, however, had an increased infectivity; hence, E2 stem region mutations increased the specific infectivity of released particles.

To determine to what extent the common H77C E1 protein was incorporated in viral particles produced for the E2 exchange recombinants, we concentrated the released particles using sucrose cushion ultracentrifugation and analyzed them by SDS-PAGE and Western blotting (WB). We could demonstrate incorporation of E1 protein for all 1b-E2 H77C/JFH1_{V787A Q1247L} recombinants (Fig. 6B). Using the amount of core for normalization, a greater amount of E1 was observed for the DH1-E2 recombinants than for J4-E2 and DH5-E2 with or without E2 stem region mutations and for H77C/JFH1_{V787A Q1247L}. Furthermore, introduction of E2 stem region mutations apparently led to an increased E1 amount within isolates for DH1-E2 with or without G706R. This clear pattern could not be confirmed in J4-E2 with or

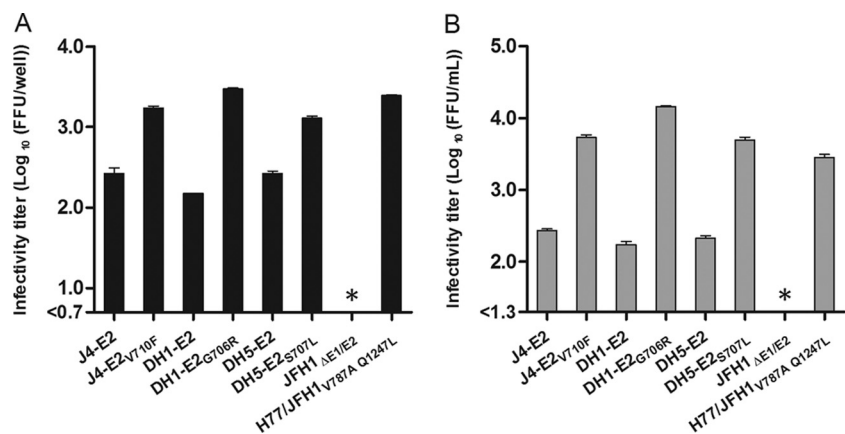


FIG 5 Intracellular (A) and extracellular (B) infectivity titers of transfected S29 cells at 48 h posttransfection. *In vitro* transcripts of 1b-E2 H77C/JFH1_{V787A Q1247L} recombinants with and without E2 compensatory mutations were transfected into S29 hepatoma cells lacking CD81. H77C/JFH1_{V787A Q1247L} and JFH1_{ΔE1/E2} were included as positive and negative controls, respectively. All measurements are presented as mean values of triplicates, with error bars displaying standard errors of the means (SEM). The lower limit of quantification was 10^{0.7} FFU/well (A) or 10^{1.3} FFU/mL (B). Samples with titers under the detection limit are indicated by an asterisk.

without V710F or in DH5-E2 with or without G706R. E2 protein could be detected only for DH1-E2 in the E2-exchanged recombinants. Like for E1, an increase in E2 incorporation was identified for DH1-E2_{G706R} compared to DH1-E2.

E1/E2 heterodimerization in 1b-E2-exchanged recombinants is not influenced by stem region mutations. Previous studies have reported E2 to be the directly interacting partner for CD81, whereas E1 cointeracts via E2 (22). Thus, we used CD81-LEL-GST-coated beads in co-IP to elucidate if the E2 stem region adaptive mutations affected E1/E2 heterodimerization and binding to the CD81-LEL. For these experiments, we used E1/E2 plasmids expressing E1 from H77 and E2 from J4, DH1, or DH5 with or without E2 stem region mutations as originally constructed for the HCVpp assays.

Immunoblotting of the co-IP elution fractions revealed the presence of E1 and E2 in J4-E2 with or without V710F, DH1-E2

with or without G706R, and DH5-E2 with or without S707L and hence confirmed the formation of functional E1/E2 heterodimers (Fig. 7A). In addition, the CD81-LEL binding was confirmed to be specific, as no H77 envelope protein could be pulled down with GST tag-coated beads. No differences in E1 or E2 level or binding to CD81-LEL were identified in the presence or absence of E2 stem region mutations within isolates. Interestingly, variation in E1/E2 heterodimer levels between isolates was present, for which DH1-E2 with or without G706R exhibited the highest degree of envelope proteins and DH5-E2 with or without S707L had significantly decreased levels of both E1 and E2. This indicates a difference in binding affinity to CD81-LEL between the E2 proteins of distinct isolates. To verify that similar amounts of E1 and E2 were expressed in transfected 293T cells with the various combinations of E2-exchanged plasmids and included controls, we also performed immunoblotting on the input lysate and found no notable

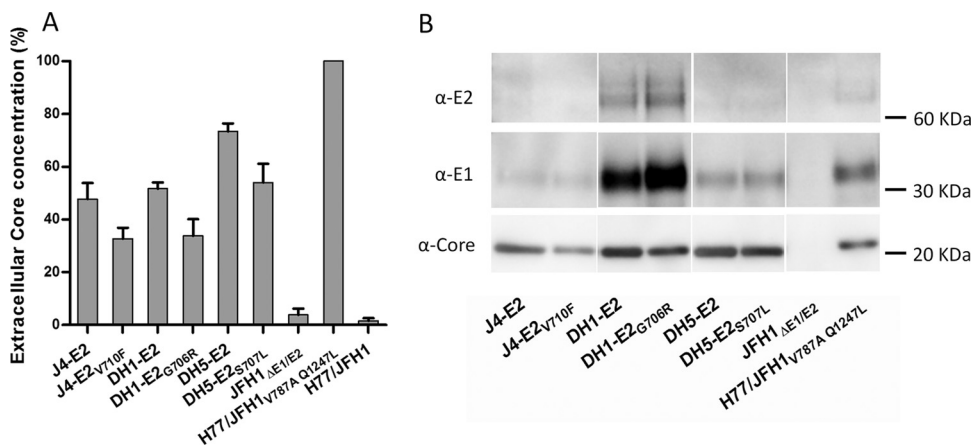


FIG 6 Influence of E2 exchange on particle assembly/release. (A) Core protein secretion of 1b-E2 H77C/JFH1_{V787A Q1247L} recombinants with or without E2 compensatory mutations was quantified in S29 cells in three independent experiments at 48 h posttransfection using ELISA. Values are presented as mean percentages of the value for the positive control, H77C/JFH1_{V787A Q1247L} (100%). Negative controls were H77C/JFH1 and JFH1_{ΔE1/E2}. Statistical significance of core concentration differences was determined using the *t* test (*P* value of <0.05 was considered significant), as stated in the text. (B) HCV release was measured by detection of extracellular core, E1, and E2 proteins in the virus supernatants collected at 48 h posttransfection of S29 cells, using SDS-PAGE and Western blotting with HCV-specific anti-core, anti-E1, or anti-E2 antibodies. Virus particles were concentrated on a 20% sucrose cushion from supernatant of cells transfected with 1b-E2 H77C/JFH1_{V787A Q1247L} recombinants with and without compensatory E2 mutations. The negative control was JFH1_{ΔE1/E2}.

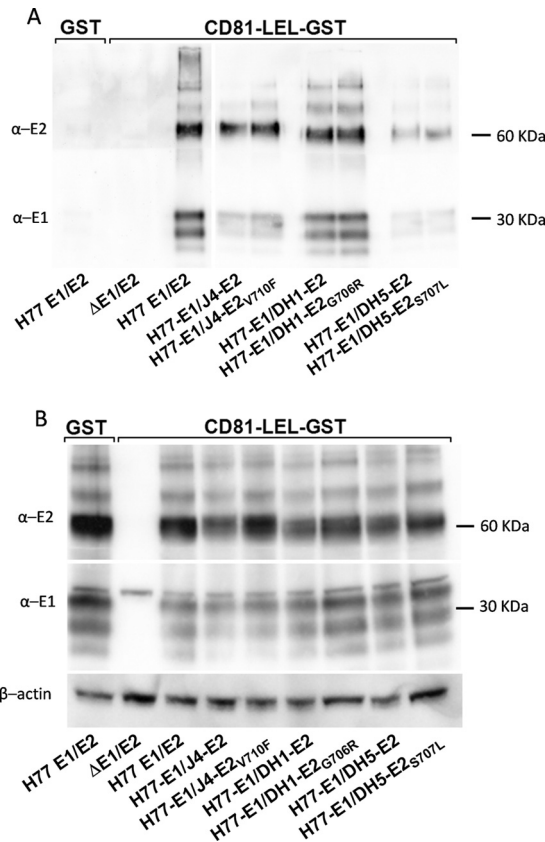


FIG 7 Influence of compensatory E2 stem region mutations on HCV E1/E2 heterodimerization. Immunoblots of elution fractions of coimmunoprecipitation using CD81-LEL-GST- or GST-tagged coated beads on lysates from transfected 293T cells (A) and of input fractions of 293T cell lysates prior to coimmunoprecipitation using anti-E1 and anti-E2 specific antibodies (B) are shown. An H77C E1/E2 positive control was transfected in duplicate and served as a specificity control, as co-IP was conducted using both CD81-LEL-GST-coated beads (H77 E1/E2) and GST-tagged coated beads only (H77 E1/E2 GST). The Δ E1/E2 construct (pHCMV-ires, in which the partial E1/E2 HCV sequence was deleted) was included as an E1/E2 negative control. β -Actin served as loading control.

differences in protein expression (Fig. 7B). Thus, introduction of stem region mutations did not influence the heterodimer formation between the E1 and E2 proteins, nor did it alter the E2 binding to CD81.

Influence of E2 stem region mutations on infectious viral particle density. We used equilibrium gradient density centrifugation to evaluate the possible influence of the E2 stem region mutations on the density of the produced infectious 1b-E2 H77C/JFH1_{V787A Q1247L} recombinant particles. We observed peak infectivity titers at densities comparable to that for the positive control for both J4-E2 and DH5-E2 recombinants with or without single compensatory mutations (Fig. 8A). However, for the original and mutated DH1-E2, the infectivity peak extended to slightly higher densities, with infectious particles detected at densities of as high as 1.15 g/ml. A significant increase in infectivity, with a slight shift in density, was observed for all three E2-exchanged recombinants harboring compensatory mutations compared to the original 1b-E2 H77C/JFH1_{V787A Q1247L} recombinants (Fig. 8A). Infectivity titers were enhanced compared to those of the original recombinants, with an average of $\sim 1.2 \log_{10}$ FFU/ml within fractions of

comparable densities. The detected peak infectivity titers for the adapted E2-exchanged recombinants ranged in density from 1.09 to 1.10 g/ml, consistent with previous *in vitro* studies (28).

To characterize the density distribution of particle-associated core, we performed core antigen ELISA on each of the density fractions (Fig. 8B). Consistent with the infectivity titration data, we observed peak core concentrations at slightly higher densities (average increase, ~ 0.2 g/ml) for the original 1b-E2 H77C/JFH1_{V787A Q1247L} recombinants compared to recombinants with compensatory mutations. The specific infectivity measured as FFU/core amount on each fraction was low, ranging from 102 to 229 FFU/fmol core, for the original E2-exchanged recombinants compared to the corresponding E2 stem region-mutated recombinants. This observation was consistent with the low titer level seen in all original E2-exchanged recombinants (Fig. 2) and the relatively high secretion of core (Fig. 6). The 1b-E2 recombinants with E2 stem region mutations had a relatively low specific infectivity at peak titer fractions. This observation was most pronounced for the DH5-E2_{S707L} recombinant (Fig. 8C). The low-density particles in general displayed the highest specific infectivity, which was consistent with previous studies showing the importance of virion-associated lipoproteins for HCV infection (28, 45).

Role of stem region mutations in HCV particle stability, host cell binding, and CD81 receptor dependence. In order to further characterize the functional role of the E2 stem region mutations, we investigated their influence on host cell binding for all 1b-E2 recombinants. In addition, HCVcc thermostability and CD81 receptor usage assays were conducted using DH5-E2 with or without S707L as a representative for the 1b-E2-exchanged isolates.

As differences in virus viability potentially could be caused by variation in particle degradation, a particle thermostability kinetics assay was established. HCVcc-containing supernatant harvested from S29 cells transfected with DH5-E2 with or without S707L was titrated following incubation at 37°C for 0 h, 4 h, 8 h, 16 h, 24 h, and 32 h (Fig. 9). Supernatants containing DH5-E2 particles with or without S707L exhibited highly similar degradation of infectious particles, with the most pronounced degradation rate in the time interval from 0 to 8 h postincubation.

As variation in both binding and receptor usage most likely would cause significant differences in virus viability, assays elucidating general host cell particle binding and dependence on the well-characterized CD81 entry factor (46) were conducted. To determine potential differences in host cell binding, supernatants from S29 cells transfected with 1b-E2-exchanged particles with or without compensatory mutations were incubated with naïve Huh7.5 cells for 2 h at 4°C, allowing particle binding. The E2 stem region mutations did not enhance binding to host cells for any of the recombinants as measured by bound HCV core amounts (Fig. 10). In addition, a dose-dependent infectivity inhibition assay was conducted on naïve Huh7.5 cells using concentrated DH5-E2 with or without S707L HCVcc, produced in S29 cells, in the presence of CD81-specific antibodies ranging from 0.004 to 2.5 μ g/ml in concentration (Fig. 11). DH5-E2 with or without S707L exhibited similar dose-response curves and IC₅₀ values (i.e., antibody concentration required for 50% inhibition) of 0.06 μ g/ml.

In summary, no significant differences in particle stability or host cell binding were present for 1b-E2-exchanged isolates with or without compensatory mutations. Additionally, we found similar CD81 receptor dependence of DH5-E2 with or without S707L.

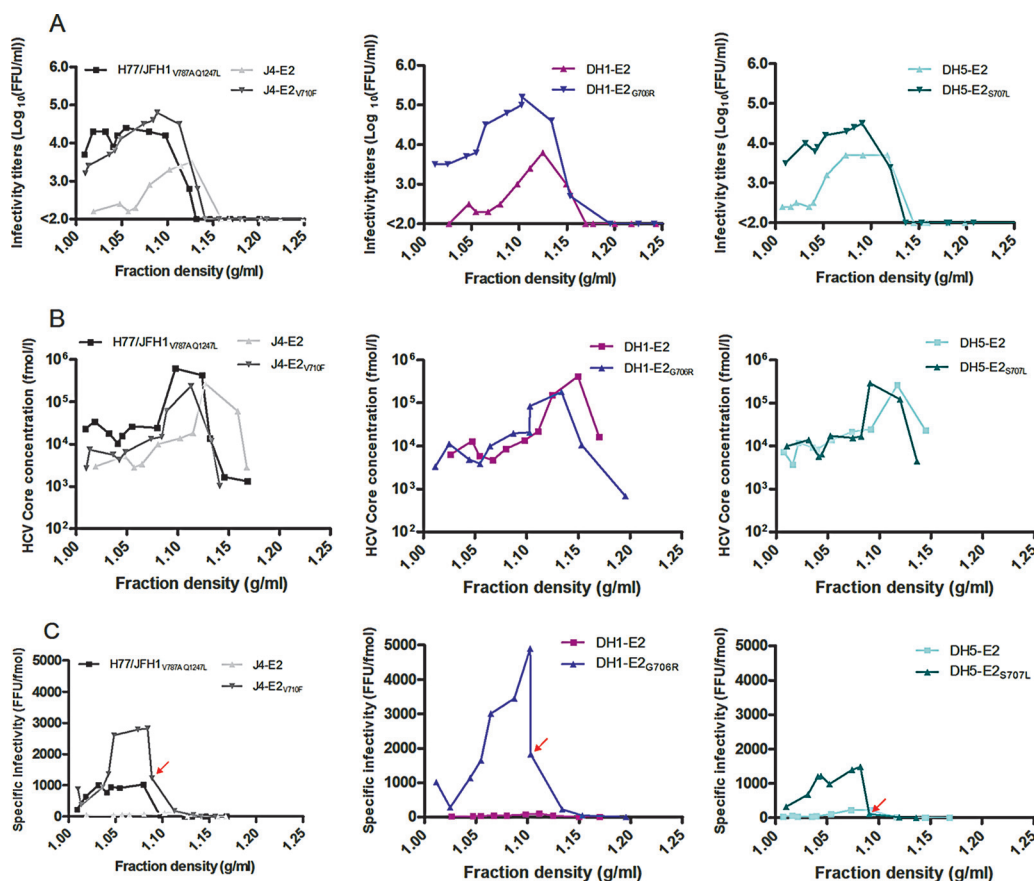


FIG 8 Density analysis of HCVcc particle infectivity (A), total core amount produced (B), and specific infectivity (C) of 1b-E2-exchanged H77C/JFH1_{V787A Q1247L} recombinants with or without compensatory E2 mutations: H77C/JFH1_{V787A Q1247L} (J4-E2) with or without V710F, H77C/JFH1_{V787A Q1247L} (DH1-E2) with or without G706R, and H77C/JFH1_{V787A Q1247L} (DH5-E2) with or without S707L. Supernatants harvested from S29 cells at 48 h posttransfection were ultracentrifuged in a 10 to 40% iodixanol gradient, and fractions were analyzed. The transfection efficiency was monitored in all cultures using NS5A-specific immunostaining prior to ultracentrifugation. The positive control was H77C/JFH1_{V787A Q1247L}. In panel A, quantified titers are presented as the mean values of triplicates, and the lower limit of detection is $10^{2.0}$ FFU/ml. In panel C, the peak titer fraction for E2-exchanged recombinants with compensatory mutations is indicated with red arrows.

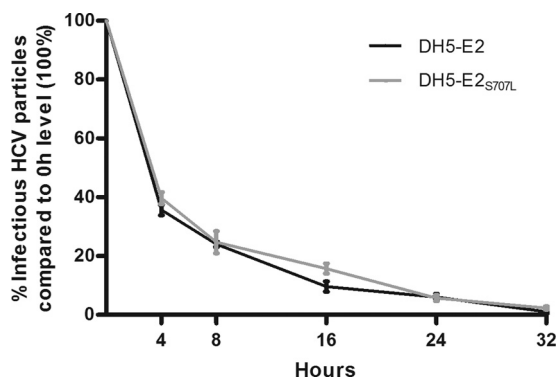


FIG 9 HCV particle stability at 37°C, analyzed during a period of 32 h. *In vitro*-generated RNA transcripts of DH5-E2 and DH5-E2_{S707L} were transfected into S29 cells for production of HCVcc. At 48 h posttransfection, particle-containing supernatant was harvested, aliquoted, and incubated at 37°C. At the indicated time points, supernatant was transferred to -80°C , followed by subsequent infectivity titration in naive Huh7.5 cells. Titer results are presented as percent infection compared to the 0-h infectivity level. Values shown are means from three independent assays, with error bars displaying standard errors of the means (SEM) between assays; for each independent assay, titrations for all time points were in triplicates.

Significant impact of G706R, S707L, and V710F compensatory mutations on HCV entry. To further elucidate the influence of the cell culture-identified E2 stem region mutations on entry, we constructed recombinant HCVpp harboring E1 from the H77C isolate and E2 from isolate J4, DH1, or DH5 with or without the E2 stem region mutations. We produced HCVpp in two independent experiments, which were used in two independent infection assays. For each HCVpp assay, H77C E1/E2 served as a positive control, whereas an empty expression vector ($\Delta\text{E1/E2}$) was included as a negative control. To correlate for intraexperiment variability, the H77C E1/E2 positive control was included in duplicates in all infection assays.

The chimeric H77C-E1/1b-E2 HCV pseudoparticles were infectious in Huh7.5 cells, although a significant increase of infectivity was observed for each isolate after introducing corresponding compensatory E2 mutations (Fig. 12A). For H77C-E1/DH1-E2_{G706R} and H77C-E1/DH5-E2_{S707L}, infectivity exceeded or was comparable to that of the H77C positive control. In contrast, the increase in infectivity for H77C-E1/J4-E2_{V710F} compared to H77C-E1/J4-E2 did not reach the level of H77C E1/E2. To quantify the increase in infectivity caused by the presence of E2 stem region mutations, we calculated the infectivity ratio between chi-

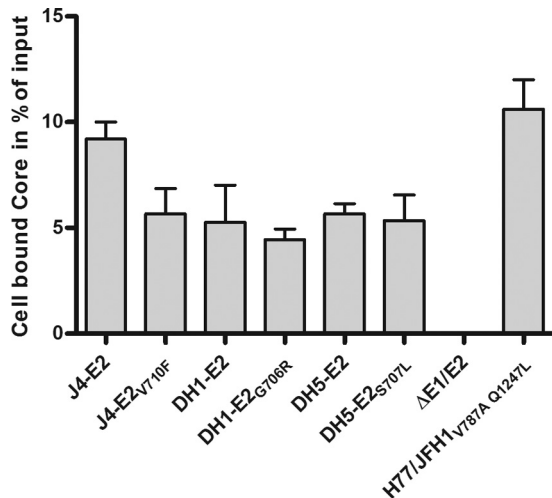


FIG 10 HCVcc particle binding assay on 1b-E2-exchanged recombinants with or without stem region mutations. *In vitro* transcripts of 1b-E2 H77C/JFH1-V787A Q1247L recombinants with and without E2 compensatory mutations were transfected into S29 cells for production of HCVcc. At 48 h posttransfection, particle-containing supernatant was harvested and an inoculum was applied to naïve Huh7.5 cells for 2 h at 4°C to allow binding but not entry of the HCVcc particles. Following incubation, cells were washed and lysed, and cell-bound core protein was quantified using core ELISA. Results are presented as cell-bound core protein in percentage of the core input for each isolate. All measurements are presented as mean values from duplicate experiments, with error bars displaying standard errors of the means (SEM). Controls were H77C/JFH1-V787A Q1247L (positive control), and JFH1-ΔE1/E2 (lacking envelope proteins).

meric HCVpp with and without compensatory mutations in the two independent experiments (Table 2). For H77C-E1/J4-E2, introduction of V710F increased infectivity of HCVpp by 4.46- and 4.21-fold. In the case of H77C-E1/DH1-E2, the recombinant harboring G706R was 3.15 and 3.46 times more infectious than the original chimeric construct, while the S707L mutation increased infectivity by 2.35- and 2.37-fold for H77C-E1/DH5-E2. The increase in infectivity was in all cases significant ($P < 0.001$).

We performed immunoblot detection of MLV capsid protein in the supernatants used for infection assays to exclude that differences in infectivity between HCVpp were due to variation in the quantity of particles produced for the assay. No differences in the amount of capsid were detected (Fig. 12B). Thus, introduction of cell culture-acquired compensatory mutation G706R, S707L, or V710F led to a significant increase in entry of H77C-E1/1b-E2 recombinant HCVpp.

The presence of E1 and E2 was identified in WB on sucrose cushion-concentrated HCVpp from collected supernatants and on the transfected 293T cell lysate. When analyzing concentrated HCVpp used for the infection assays, we observed that E1, as well as E2, was incorporated into the particles. For each chimeric E1/E2 HCVpp, similar amounts of E1 were incorporated in particles with and without compensatory mutations (Fig. 12B). When comparing E1 amounts between isolates, however, H77C-E1/J4-E2 and H77C-E1/DH5-E2 had significantly decreased levels incorporated compared to H77C-E1/DH1-E2 and the H77C E1/E2 control. This was consistent with findings in HCVcc particles (Fig. 6B). We observed less incorporation of E2 into H77C-E1/DH1-E2-G706R and H77C-E1/DH5-E2-S707L compared with the chimeric particles without mutations. This was not caused by a

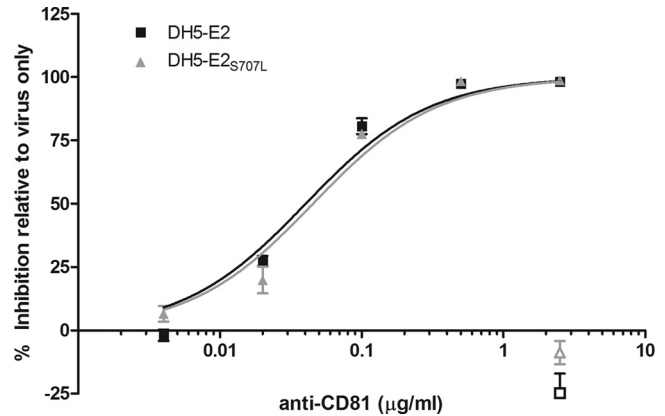


FIG 11 Dose-dependent inhibition of DH5-E2 with or without S707L binding to the CD81 receptor using CD81 specific antibody. *In vitro*-generated RNA transcripts of DH5-E2 and DH5-E2-S707L were transfected into S29 cells for production of HCVcc. At 48 h posttransfection, particle-containing supernatant was harvested and DH5-E2 with or without S707L inoculum was applied to naïve Huh7.5 cells which had been incubated with anti-CD81 antibody at concentrations ranging from 0.004 to 2.5 μg/ml for 1 h preinfection. Results are presented as the means of 4 replicates at each antibody concentration, with error bars representing SEM. Percent inhibition was calculated relative to infectivity titers of 6 replicates of virus only. Open symbols represent percent inhibition relative to virus only using an isotype-matched negative control at a concentration of 2.5 μl/ml.

lower expression of E2 in the transfected 293T cells with the respective plasmids (Fig. 12C). Comparison of the incorporation of E2 between the different HCVpp constructs was not possible due to possible differences in antibody affinity between isolates.

In conclusion, these data showed that mutations G706R, S707L, and V710F in the E2 stem region increased entry and thus compensated for the decreased infectivity of the 1a-E1/1b-E2 envelope-chimeric particles.

DISCUSSION

In this study, we investigated the role of the E1/E2 heterodimer during the HCV life cycle and further analyzed the function of a five-amino-acid stretch in the E2 stem region that is essential for the function of the envelope proteins. By exchanging the E2 gene of a previously developed 1a (H77 core-NS2)/2a JFH1-based recombinant with the corresponding gene from genotype 1a, 1b, or 2a isolates, we found very different effects on viral viability. Although exchange of E2 with that of a different isolate from the same subtype (TN) conferred immediate viral spread without the need for compensatory mutations, no viral recovery was observed when exchanging E2 from a different genotype (J6, genotype 2a) (Fig. 1). Interestingly, when exchanging E2 from another subtype (J4, DH1, and DH5, genotype 1b), spread of infection was delayed. We identified single mutations within aa 706 to 710 of the E2 stem region in the recovered 1b-E2 recombinant viruses. Introduction of these mutations increased viral titers on average ~100-fold, confirming a compensatory effect.

The identified mutations, i.e., V710F or V710G in J4-E2, G706R in DH1-E2, and S707L in DH5-E2 (Table 1), were analyzed in a multiple-sequence alignment containing 513 HCV E2 sequences from genotype 1 (44) (see Fig. S1 in the supplemental material, and data not shown). S707 was conserved in all genotype 1 sequences, and the same was observed in subtype 1a and 1b for

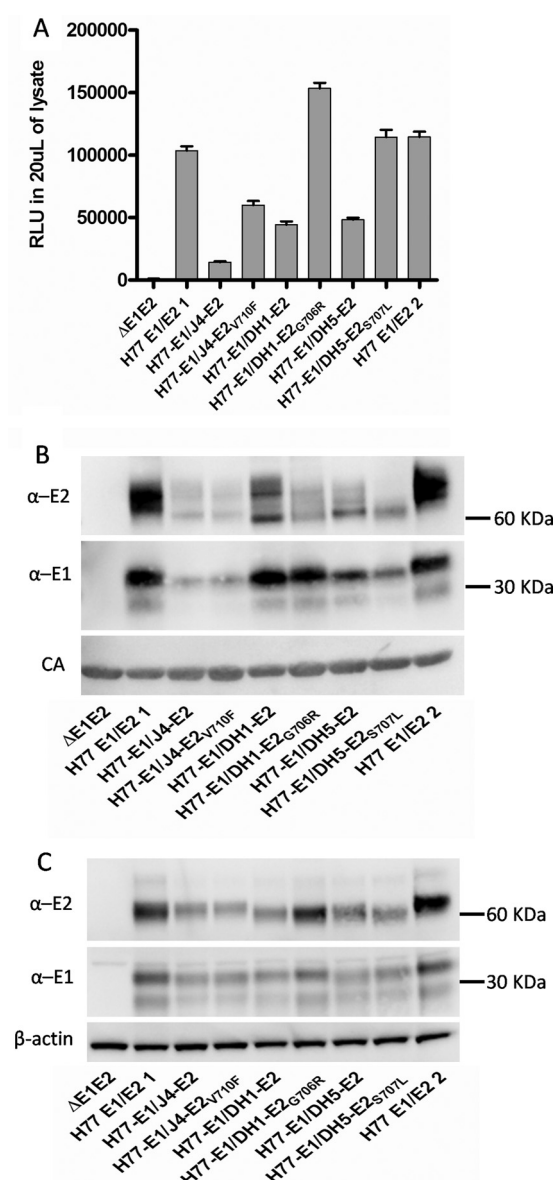


FIG 12 Effect of compensatory E2 mutations on chimeric HCV pseudoparticle entry. (A) Infectivity of HCVpp was detected by luciferase reporter gene expression. Infectivity is presented in relative light units (RLU) obtained in 20 μ l of cell lysate from a representative experiment. Error bars show the standard errors of the means (SEM) of 8 replicates. (B and C) Immunoblots of concentrated HCVpp (B) and HCVpp 293T cell lysate (C) using anti-E1 and anti-E2 specific antibodies, originating from the experiment presented in panel A. The H77C E1/E2 positive control was transfected in duplicates and served as an intraexperiment control. The Δ E1/E2 construct (pCMV-ires in which the HCV sequence was deleted) was included as a negative control. Anti- β -actin and anti-Gag MLV (CA) were included as loading controls.

G706, although subtype 1c had S706. At position 710, the amino acid distribution was more heterogeneous, with genotype 1 sequences containing V (~67%), A (~30%), T (~3%), or I (<1%). Interestingly, none of the sequences included in the alignment contained the residue 706R, 707L, 710F, or 710G, which we identified from the recovered 1b-E2-exchanged viruses. When analyzing the influence of the G706R, S707L, and V710F mutations on viability separately for all 1b-E2 H77C/JFH1_{V787A Q1247L} recombinants,

we found the J4-E2 and DH1-E2 functionality to be dependent on the mutations originally identified for these particular recombinants (V710F and G706R, respectively) (Fig. 2D). In contrast, introduction of the three E2 stem region mutations independently into DH5-E2 resulted in immediate viral spread following transfection of these mutants and production of robust infectivity titers. These observations suggested that the unique E2 stem region mutations compensated for the attenuated phenotype of the original 1b-E2 recombinants, primarily impacting the E2 from which the specific mutation was identified.

The fact that the TN-, J4-, DH1-, DH5-, and J6-E2 proteins are all functional in the JFH1-based core-NS2 recombinant from which they were derived (31, 32, 34, 35) indicates the existence of a genotype-specific interaction between E2 and core, E1, p7, or NS2. Given our findings, particularly in the pseudoparticle system, it seems likely that the functional incompatibilities of the E2-exchanged recombinants are caused by a coevolution of E1 and E2, thereby creating a genotype-specific interaction that to a lesser extent also applies to subtypes, and, furthermore, that the E2 stem region plays an important role in this interaction. Identification of single E1 mutations which in two E2-exchanged isolates fully restored viability (Fig. 3) suggested that mutations in E1 compensated either directly for a change in the E1/E2 interaction or indirectly for that of the E1/E2 heterodimer with a third molecule such as a cellular entry factor.

We demonstrated that chimeric H77-E1/1b-E2 HCVpp, although able to enter Huh7.5 cells, have impaired infectivity compared to H77C E1/E2. Others have reported functional chimeric H77C-E1/1b-E2 (Con1 isolate) HCVpp being able to reach infectivity levels comparable to those for the H77 E1/E2 control (47). These differences in infectivity between H77C-E1/1b-E2 chimeras might be explained by the entry efficiency differences in the genotype 1b isolates used, even though we observed decreased entry for all three 1b isolates. It should be noted that in contrast to our HCVpp infection assays, which were performed with Huh7.5 target cells to better correlate results with the HCVcc data, the previously published study used the original Huh7 target cells (47).

While we were not able to adapt the intergenotypic 1a/2a HCVcc construct with E2 from J6, two previous studies report intergenotypic H77C-E1/E2 combinations to be functional for entry, concluding that H77C-E1 is compatible with E2 from the same and different genotypes in the HCVpp system (25, 47). We speculate that in the HCVcc context, other factors in the HCV life cycle besides entry play an important role in the intergenotypic incompatibility observed here. We cannot rule out, however, that

TABLE 2 Infectivity of chimeric HCVpp with or without compensatory mutations in two independent experiments^a

HCVpp	Mean ratio, 95% confidence limit (<i>P</i> value ^b) in expt:	
	1	2
H77-E1/E2-J4 _{V710F} vs H77-E1/E2-J4	4.46, 3.32–6.01 (< 0.001)	4.21, 3.62–4.9 (< 0.001)
H77-E1/E2-DH1 _{G706R} vs H77-E1/E2-DH1	3.15, 2.67–3.72 (< 0.001)	3.46, 3.03–3.95 (< 0.001)
H77-E1/E2-DH5 _{S707L} vs H77-E1/E2-DH5	2.35, 2.01–2.74 (< 0.001)	2.37, 2.11–2.65 (< 0.001)

^a Luciferase measurement was used as a measure of infectivity.
^b The statistical significance of the differences was tested with the Wilcoxon rank sum test, and a *P* value of less than 0.005 was considered statistically significant.

this is a result of the recognized differences between the HCVpp and HCVcc systems with regard to entry (22).

We used the CD81-deficient S29 cell single-cycle assay to investigate the impact of the E2 stem region mutations on replication and assembly/release. Introduction of compensatory mutations did not influence replication (Fig. 4). This was expected, since only NS3-NS5B is required for replication (14). In contrast, compared to that for H77C/JFH1_{V787A Q1247L}, exchange of the E2 gene resulted in a significant decrease of core release for all 1b-E2 H77C/JFH1_{V787A Q1247L} recombinants, with this decrease being different in the distinct isolates tested (Fig. 6A). The different levels of decrease in core release could be explained by the heterogeneity within the E2 ectodomain, given the importance of the E2 ectodomain for viral assembly (48, 49). Following introduction of compensatory E2 stem region mutations in 1b-E2-exchanged recombinants, we observed a further reduction in the release of core protein compared to that for the original 1b-E2 H77C/JFH1_{V787A Q1247L}. Thus, the single compensatory E2 mutations seemed to increase the infectivity of viral particles at the expense of core release, thereby increasing the specific infectivity of the virus.

We observed variations in the levels of incorporation of E1 in both HCVpp and HCVcc between isolates when exchanging the E2 gene. Reduced E1 incorporation levels were most pronounced when exchanging E2 with J4 or DH5 isolates (Fig. 6B and 12B). Interestingly, the degree of envelope protein integration did not correlate with differences in infectivity following introduction of the E2 compensatory mutations, as peak infectivity titers between isolates were comparable (Fig. 2). Thus, the amount of envelope protein on the virus particle did not seem to be the limiting factor for production of infectious virus from the original E2 exchange recombinants. In the HCVpp system, a previous study reported increased particle infectivity concomitantly with increasing amounts of incorporated E1 and E2 (50), although this finding cannot be directly compared to our E2-exchanged recombinants with and without compensatory mutation, as other factors, e.g., protein heterodimerization or proper protein folding, could be the limiting factor for infectivity. However, the co-IP CD81-LEL analysis on all H77-E1/1b-E2 recombinants indicated that heterodimerization was maintained following E2 exchange. In agreement with the HCVcc and HCVpp results, the DH1-E2 recombinant with or without G706R had increased envelope protein amounts compared to those of J4-E2 and DH5-E2 (Fig. 6, 7, and 12). This points toward increased heterodimerization ability within H77-E1/DH1-E2 resulting in increased glycoprotein incorporated in the particle or improved CD81 affinity of the DH1-E2 protein. Interestingly, we furthermore found no influence of E2 stem region mutations on the degree of heterodimerization within isolates (Fig. 7). This preserved heterodimerization ability was supported by a previous study investigating specific E2 domains (25).

As introduction of the E2 stem region mutations did not enhance intracellular heterodimerization or the release of virus particles as measured by the levels of core, E1, and E2, despite an ~2-log increase in infectivity, we decided to investigate the impact of the mutations on viral particle stability, host cell binding, and CD81 receptor usage. However, none of these were increased by introduction of E2 stem region mutations. The results resembled those from previous reports on the particle thermostability degradation rate (51) and CD81 receptor dependency for efficient infection (31). Our combined data suggest that the E2 stem region

mutations primarily influence steps downstream of the CD81 receptor interaction in the HCV entry pathway.

Several HCVpp studies have shown that heterodimerization of E1 and E2 is a requirement to obtain infectious HCVpp (26, 52, 53). Thus, the co-IP results correlated with the observation that infectious HCVpp was produced for all H77-E1/1b-E2 chimeras with or without E2 stem region mutations. Interestingly, introduction of V710F, G706R, and S707L into the corresponding chimeric pseudoparticles H77C-E1/J4-E2, H77C-E1/DH1-E2, and H77C-E1/DH5-E2, respectively, resulted in an average >3-fold increase in infectivity (Table 2 and Fig. 12). Our results are supported by a previous study highlighting functional regions of the E2 glycoprotein, including the importance of the stem region for HCV entry (25). In the previous study, a 2.5-log titer decrease was observed in the JFH1 genotype 2a infectious cell culture system following exchange of aa 705 to 715 in the E2 stem region with the corresponding sequence of a genotype 1a isolate. In addition, attempts to identify specific stem region residues important for infectivity in a wild-type 2a virus were made. However, none of the tested mutations, including mutations at aa 707 and aa 710, influenced virus viability (25). In immunoblot detection of E2 in both co-IP and HCVpp assays, we found that intracellular E2 from DH1 and DH5 migrated at a smaller protein size than J4 E2 (Fig. 7 and Fig. 12C). Through amino acid sequence analysis, we identified the presence of 11 previously described N-linked glycosylation sites (54) in J4-E2, whereas only 10 sites were found in DH1 and DH5 (i.e., glycosylation site 5 [aa 478] was absent). Thus, the difference in protein size could potentially be caused by the absence of this N-linked glycosylation site. However, considering the location of the glycosylation difference and the fact that no differences in infectivity between isolates were observed, we find this unlikely to have an influence on the function of the E2 stem region mutations. The lack of influence on infectivity and heterodimerization of E2 glycosylation site 5 was confirmed in a previous study (55).

Based on the heterodimerization and HCVpp results, chimeric E1 and E2 form functional heterodimers able to bind to CD81, which is not increased by E2 stem region mutations. The mutations identified in our study could act at a later step in entry; one possibility is that they induce conformational changes in the stem region, thereby increasing the functionality of the E1/E2 complex and possibly resulting in an improved unshielding of host cell receptor binding sites or fusogenic domains in late steps of the HCV entry pathway. A previous study has proposed that the stem region has an influence on envelope protein reorganization during the fusion process (56). Thus, E2 stem region mutations could favor a direct reestablishment of correct envelope protein interaction.

Interestingly, when performing equilibrium gradient density centrifugation for physicochemical analysis of the produced particles, we observed a tendency for peak infectivity titers and peak core levels at slightly higher densities for the original E2-exchanged recombinants in comparison with the positive control and the mutant 1b-E2 recombinants (Fig. 8A and B). This could be due to the high production of noninfectious particles, which might fail to interact with a sufficient amount of lipids, thus increasing their density. Previous studies have elucidated the importance of lipoprotein association to HCV particles in relation to an increased specific infectivity (45, 57); hence, a decrease in this association could give rise to the low specific infectivity in the

original 1b-E2-exchanged recombinants (Fig. 8C). We furthermore observed a low specific infectivity in all E2-exchanged recombinants at the densities with peak infectivity titers, indicating the presence of large amounts of noninfectious particles in these fractions (Fig. 8C). This was in agreement with findings from other groups, where densities with peak RNA titers correlated to low specific infectivity (58–60). In general, the highest specific infectivity was found in the low-density fractions, in agreement with previous findings (22). Therefore, it cannot be excluded that the viability increase for the mutated 1b-E2 recombinants could be caused indirectly through increased interaction of virion-associated lipid with host cell receptors.

In future studies, it would be of interest to further study host receptor binding, especially at late steps of the HCV entry process, to investigate where the identified mutations in the E2 stem region have specific influence on host cell receptor interaction and thus on virus particle uptake. In addition, it would be of relevance to examine the importance of the E2 stem region using similar approaches for other HCV genotypes.

In summary, we have used a genetic and biochemical strategy to characterize the HCV E1 and E2 glycoprotein function in context of the complete virus life cycle, aiming at a better understanding of their role in HCV infection. To our knowledge, this study is the first to identify single amino acid residues in the E2 stem region with functional importance for viral entry. Further knowledge about residues important for HCV entry could be important for HCV disease and control, as the envelope proteins might constitute a valuable target for future therapy. Furthermore, a better understanding of the HCV envelope protein functionality could have impact on the design of antibody-based HCV vaccine or prophylaxis.

ACKNOWLEDGMENTS

We thank Lotte Mikkelsen for technical assistance, Anna-Louise Sørensen for laboratory support, and Steen Ladelund for statistical advice. We also thank Jens Ole Nielsen and Ove Andersen (Copenhagen University Hospital, Hvidovre, Denmark) for supporting this study and Suzanne Emerson and Robert Purcell (National Institutes of Health, Bethesda, MD), Charles Rice (Rockefeller University, New York, NY), Jean Dubuisson (Institut Pasteur de Lille, Lille, France), François-Loïc Cosset (Université de Lyon, Lyon, France), and Akito Sakai (Kanazawa University, Kanazawa, Japan) for providing reagents.

This study was supported by Ph.D. stipends from the Faculty of Health Science, University of Copenhagen (T.H.R.C. and T.K.H.S) and individual postdoctoral stipends from the Danish Council for Independent Research, Medical Sciences (T.K.H.S and S.R.). Other research grants were from the Lundbeck Foundation (T.K.H.S and J.B.), The Danish Cancer Society (T.H.R.C and J.B.), Novo Nordisk Foundation (J.B.), The Danish Medical Research Council (J.B.), and A. P. Moeller and the Chastine McKinney Moeller Foundation (T.K.H.S. and J.B.).

We have no conflicts of interest.

REFERENCES

- Pawlotsky JM. 2004. Pathophysiology of hepatitis C virus infection and related liver disease. *Trends Microbiol.* 12:96–102.
- Sarrazin C, Hezode C, Zeuzem S, Pawlotsky JM. 2012. Antiviral strategies in hepatitis C virus infection. *J. Hepatol.* 56(Suppl. 1):S88–S100.
- Manns MP, Wedemeyer H, Cornberg M. 2006. Treating viral hepatitis C: efficacy, side effects, and complications. *Gut* 55:1350–1359.
- Angus AG, Patel AH. 2011. Immunotherapeutic potential of neutralizing antibodies targeting conserved regions of the HCV envelope glycoprotein E2. *Future Microbiol.* 6:279–294.
- Syder AJ, Lee H, Zeisel MB, Grove J, Soulier E, Macdonald J, Chow S, Chang J, Baumert TF, McKeating JA, McKelvey J, Wong-Staal F. 2011. Small molecule scavenger receptor BI antagonists are potent HCV entry inhibitors. *J. Hepatol.* 54:48–55.
- Zeisel MB, Fofana I, Fafi-Kremer S, Baumert TF. 2011. Hepatitis C virus entry into hepatocytes: molecular mechanisms and targets for antiviral therapies. *J. Hepatol.* 54:566–576.
- Baldick CJ, Wichroski MJ, Pendri A, Walsh AW, Fang J, Mazzucco CE, Pokornowski KA, Rose RE, Eggers BJ, Hsu M, Zhai W, Zhai G, Gerritz SW, Poss MA, Meanwell NA, Cockett MI, Tenney DJ. 2010. A novel small molecule inhibitor of hepatitis C virus entry. *PLoS Pathog.* 6:e1001086. doi:10.1371/journal.ppat.1001086.
- Ciesek S, von Colpitts HTCC, Schang LM, Friesland M, Steinmann J, Manns MP, Ott M, Wedemeyer H, Meuleman P, Pietschmann T, Steinmann E. 2011. The green tea polyphenol, epigallocatechin-3-gallate, inhibits hepatitis C virus entry. *Hepatology* 54:1947–1955.
- Helle F, Goffard A, Morel V, Duverlie G, McKeating J, Keck ZY, Foug S, Penin F, Dubuisson J, Voisset C. 2007. The neutralizing activity of anti-hepatitis C virus antibodies is modulated by specific glycans on the E2 envelope protein. *J. Virol.* 81:8101–8111.
- Helle F, Wychowski C, Vu-Dac N, Gustafson KR, Voisset C, Dubuisson J. 2006. Cyanovirin-N inhibits hepatitis C virus entry by binding to envelope protein glycans. *J. Biol. Chem.* 281:25177–25183.
- Keck ZY, Saha A, Xia J, Wang Y, Lau P, Krey T, Rey FA, Foug SK. 2011. Mapping a region of hepatitis C virus E2 that is responsible for escape from neutralizing antibodies and a core CD81-binding region that does not tolerate neutralization escape mutations. *J. Virol.* 85:10451–10463.
- Law M, Maruyama T, Lewis J, Giang E, Tarr AW, Stamatakis Z, Gastaminza P, Chisari FV, Jones IM, Fox RI, Ball JK, McKeating JA, Kneteman NM, Burton DR. 2008. Broadly neutralizing antibodies protect against hepatitis C virus quasispecies challenge. *Nat. Med.* 14:25–27.
- Owsianka AM, Tarr AW, Keck ZY, Li TK, Witteveldt J, Adair R, Foug SK, Ball JK, Patel AH. 2008. Broadly neutralizing human monoclonal antibodies to the hepatitis C virus E2 glycoprotein. *J. Gen. Virol.* 89:653–659.
- Moradpour D, Penin F, Rice CM. 2007. Replication of hepatitis C virus. *Nat. Rev. Microbiol.* 5:453–463.
- Bukh J, Purcell RH, Miller RH. 1993. At least 12 genotypes of hepatitis C virus predicted by sequence analysis of the putative E1 gene of isolates collected worldwide. *Proc. Natl. Acad. Sci. U. S. A.* 90:8234–8238.
- Murphy D, Chamberland J, Dandavino R, Sablon E. 2007. A new genotype of hepatitis C virus originated from central Africa. *Hepatology* 46:623A.
- Simmonds P. 2004. Genetic diversity and evolution of hepatitis C virus—15 years on. *J. Gen. Virol.* 85:3173–3188.
- Simmonds P, Bukh J, Combet C, Deleage G, Enomoto N, Feinstone S, Halfon P, Inchauspe G, Kuiken C, Maertens G, Mizokami M, Murphy DG, Okamoto H, Pawlotsky JM, Penin F, Sablon E, Shin I, Stuyver LJ, Thiel HJ, Viazov S, Weiner AJ, Widell A. 2005. Consensus proposals for a unified system of nomenclature of hepatitis C virus genotypes. *Hepatology* 42:962–973.
- Reed KE, Rice CM. 2000. Overview of hepatitis C virus genome structure, polyprotein processing, and protein properties. *Curr. Top. Microbiol. Immunol.* 242:55–84.
- Op De Beeck A, Cocquerel L, Dubuisson J. 2001. Biogenesis of hepatitis C virus envelope glycoproteins. *J. Gen. Virol.* 82:2589–2595.
- Op De Beeck A, Voisset C, Bartosch B, Ciczora Y, Cocquerel L, Keck Z, Foug S, Cosset FL, Dubuisson J. 2004. Characterization of functional hepatitis C virus envelope glycoproteins. *J. Virol.* 78:2994–3002.
- Vieyres G, Thomas X, Descamps V, Duverlie G, Patel AH, Dubuisson J. 2010. Characterization of the envelope glycoproteins associated with infectious hepatitis C virus. *J. Virol.* 84:10159–10168.
- Op De Beeck A, Montserret R, Duvert S, Cocquerel L, Cacan R, Barberot B, Le MM, Penin F, Dubuisson J. 2000. The transmembrane domains of hepatitis C virus envelope glycoproteins E1 and E2 play a major role in heterodimerization. *J. Biol. Chem.* 275:31428–31437.
- Drummer HE, Pombourios P. 2004. Hepatitis C virus glycoprotein E2 contains a membrane-proximal heptad repeat sequence that is essential for E1E2 glycoprotein heterodimerization and viral entry. *J. Biol. Chem.* 279:30066–30072.
- Albecka A, Montserret R, Krey T, Tarr AW, Diesis E, Ball JK, Descamps V, Duverlie G, Rey F, Penin F, Dubuisson J. 2011. Identification of new

- functional regions in hepatitis C virus envelope glycoprotein E2. *J. Virol.* 85:1777–1792.
26. Bartosch B, Dubuisson J, Cosset FL. 2003. Infectious hepatitis C virus pseudo-particles containing functional E1-E2 envelope protein complexes. *J. Exp. Med.* 197:633–642.
 27. Hsu M, Zhang J, Flint M, Logvinoff C, Cheng-Mayer C, Rice CM, McKeating JA. 2003. Hepatitis C virus glycoproteins mediate pH-dependent cell entry of pseudotyped retroviral particles. *Proc. Natl. Acad. Sci. U. S. A.* 100:7271–7276.
 28. Lindenbach BD, Evans MJ, Syder AJ, Wolk B, Tellinghuisen TL, Liu CC, Maruyama T, Hynes RO, Burton DR, McKeating JA, Rice CM. 2005. Complete replication of hepatitis C virus in cell culture. *Science* 309:623–626.
 29. Wakita T, Pietschmann T, Kato T, Date T, Miyamoto M, Zhao Z, Murthy K, Habermann A, Krausslich HG, Mizokami M, Bartenschlager R, Liang TJ. 2005. Production of infectious hepatitis C virus in tissue culture from a cloned viral genome. *Nat. Med.* 11:791–796.
 30. Gottwein JM, Scheel TK, Hoegh AM, Lademann JB, Eugen-Olsen J, Lisby G, Bukh J. 2007. Robust hepatitis C genotype 3a cell culture releasing adapted intergenotypic 3a/2a (S52/JFH1) viruses. *Gastroenterology* 133:1614–1626.
 31. Gottwein JM, Scheel TK, Jensen TB, Lademann JB, Prentoe JC, Knudsen ML, Hoegh AM, Bukh J. 2009. Development and characterization of hepatitis C virus genotype 1–7 cell culture systems: role of CD81 and scavenger receptor class B type I and effect of antiviral drugs. *Hepatology* 49:364–377.
 32. Scheel TK, Gottwein JM, Carlsen TH, Li YP, Jensen TB, Spengler U, Weis N, Bukh J. 2011. Efficient culture adaptation of hepatitis C virus recombinants with genotype-specific core-NS2 by using previously identified mutations. *J. Virol.* 85:2891–2906.
 33. Scheel TK, Gottwein JM, Jensen TB, Prentoe JC, Hoegh AM, Alter HJ, Eugen-Olsen J, Bukh J. 2008. Development of JFH1-based cell culture systems for hepatitis C virus genotype 4a and evidence for cross-genotype neutralization. *Proc. Natl. Acad. Sci. U. S. A.* 105:997–1002.
 34. Sakai A, Takikawa S, Thimme R, Meunier JC, Spangenberg HC, Govindarajan S, Farci P, Emerson SU, Chisari FV, Purcell RH, Bukh J. 2007. In vivo study of the HC-TN strain of hepatitis C virus recovered from a patient with fulminant hepatitis: RNA transcripts of a molecular clone (pHC-TN) are infectious in chimpanzees but not in Huh7.5 cells. *J. Virol.* 81:7208–7219.
 35. Yanagi M, Purcell RH, Emerson SU, Bukh J. 1999. Hepatitis C virus: an infectious molecular clone of a second major genotype (2a) and lack of viability of intertypic 1a and 2a chimeras. *Virology* 262:250–263.
 36. Russell RS, Meunier JC, Takikawa S, Faulk K, Engle RE, Bukh J, Purcell RH, Emerson SU. 2008. Advantages of a single-cycle production assay to study cell culture-adaptive mutations of hepatitis C virus. *Proc. Natl. Acad. Sci. U. S. A.* 105:4370–4375.
 37. Li YP, Gottwein JM, Scheel TK, Jensen TB, Bukh J. 2011. MicroRNA-122 antagonism against hepatitis C virus genotypes 1–6 and reduced efficacy by host RNA insertion or mutations in the HCV 5′ UTR. *Proc. Natl. Acad. Sci. U. S. A.* 108:4991–4996.
 38. Scheel TK, Gottwein JM, Mikkelsen LS, Jensen TB, Bukh J. 2011. Recombinant HCV variants with NS5A from genotypes 1–7 have different sensitivities to an NS5A inhibitor but not interferon- α . *Gastroenterology* 140:1032–1042.
 39. Callens N, Ciczora Y, Bartosch B, Vu-Dac N, Cosset FL, Pawlotsky JM, Penin F, Dubuisson J. 2005. Basic residues in hypervariable region 1 of hepatitis C virus envelope glycoprotein e2 contribute to virus entry. *J. Virol.* 79:15331–15341.
 40. Pestka JM, Zeisel MB, Blaser E, Schurmann P, Bartosch B, Cosset FL, Patel AH, Meisel H, Baumert J, Viazov S, Rispeter K, Blum HE, Roggendorf M, Baumert TF. 2007. Rapid induction of virus-neutralizing antibodies and viral clearance in a single-source outbreak of hepatitis C. *Proc. Natl. Acad. Sci. U. S. A.* 104:6025–6030.
 41. Keck ZY, Xia J, Wang Y, Wang W, Krey T, Prentoe J, Carlsen T, Li AY, Patel AH, Lemon SM, Bukh J, Rey FA, Fong SK. 2012. Human monoclonal antibodies to a novel cluster of conformational epitopes on HCV E2 with resistance to neutralization escape in a genotype 2a isolate. *PLoS Pathog.* 8:e1002653. doi:10.1371/journal.ppat.1002653.
 42. Dubuisson J, Hsu HH, Cheung RC, Greenberg HB, Russell DG, Rice CM. 1994. Formation and intracellular localization of hepatitis C virus envelope glycoprotein complexes expressed by recombinant vaccinia and Sindbis viruses. *J. Virol.* 68:6147–6160.
 43. Tamura K, Dudley J, Nei M, Kumar S. 2007. MEGA4: Molecular Evolutionary Genetics Analysis (MEGA) software version 4.0. *Mol. Biol. Evol.* 24:1596–1599.
 44. Kuiken C, Yusim K, Boykin L, Richardson R. 2005. The Los Alamos hepatitis C sequence database. *Bioinformatics* 21:379–384.
 45. Haid S, Pietschmann T, Pecheur EI. 2009. Low pH-dependent hepatitis C virus membrane fusion depends on E2 integrity, target lipid composition, and density of virus particles. *J. Biol. Chem.* 284:17657–17667.
 46. Cormier EG, Tsamis F, Kajumo F, Durso RJ, Gardner JP, Dragic T. 2004. CD81 is an entry coreceptor for hepatitis C virus. *Proc. Natl. Acad. Sci. U. S. A.* 101:7270–7274.
 47. Maurin G, Fresquet J, Granio O, Wychowski C, Cosset FL, Lavillette D. 2011. Identification of interactions in the E1E2 heterodimer of hepatitis C virus important for cell entry. *J. Biol. Chem.* 286:23865–23876.
 48. Bianchi A, Crotta S, Brazzoli M, Fong SK, Merola M. 2011. Hepatitis C virus e2 protein ectodomain is essential for assembly of infectious virions. *Int. J. Hepatol.* 2011:968161.
 49. McCaffrey K, Gouklani H, Boo I, Pombourios P, Drummer HE. 2011. The variable regions of hepatitis C virus glycoprotein E2 have an essential structural role in glycoprotein assembly and virion infectivity. *J. Gen. Virol.* 92:112–121.
 50. Sandrin V, Boulanger P, Penin F, Granier C, Cosset FL, Bartosch B. 2005. Assembly of functional hepatitis C virus glycoproteins on infectious pseudoparticles occurs intracellularly and requires concomitant incorporation of E1 and E2 glycoproteins. *J. Gen. Virol.* 86:3189–3199.
 51. Song H, Li J, Shi S, Yan L, Zhuang H, Li K. 2010. Thermal stability and inactivation of hepatitis C virus grown in cell culture. *Virol. J.* 7:40.
 52. Ciczora Y, Callens N, Penin F, Pecheur EI, Dubuisson J. 2007. Transmembrane domains of hepatitis C virus envelope glycoproteins: residues involved in E1E2 heterodimerization and involvement of these domains in virus entry. *J. Virol.* 81:2372–2381.
 53. Drummer HE, Maerz A, Pombourios P. 2003. Cell surface expression of functional hepatitis C virus E1 and E2 glycoproteins. *FEBS Lett.* 546:385–390.
 54. Goffard A, Dubuisson J. 2003. Glycosylation of hepatitis C virus envelope proteins. *Biochimie* 85:295–301.
 55. Goffard A, Callens N, Bartosch B, Wychowski C, Cosset FL, Montpellier C, Dubuisson J. 2005. Role of N-linked glycans in the functions of hepatitis C virus envelope glycoproteins. *J. Virol.* 79:8400–8409.
 56. Krey T, d’Alayer J, Kikuti CM, Saulnier A, Damier-Piolle L, Petitpas I, Johansson DX, Tawar RG, Baron B, Robert B, England P, Persson MA, Martin A, Rey FA. 2010. The disulfide bonds in glycoprotein E2 of hepatitis C virus reveal the tertiary organization of the molecule. *PLoS Pathog.* 6:e1000762. doi:10.1371/journal.ppat.1000762.
 57. Gastaminza P, Dryden KA, Boyd B, Wood MR, Law M, Yeager M, Chisari FV. 2010. Ultrastructural and biophysical characterization of hepatitis C virus particles produced in cell culture. *J. Virol.* 84:10999–11009.
 58. Fujita N, Kaito M, Ishida S, Nakagawa N, Ikoma J, Adachi Y, Watanabe S. 2001. Paraformaldehyde protects of hepatitis C virus particles during ultracentrifugation. *J. Med. Virol.* 63:108–116.
 59. Heller T, Saito S, Auerbach J, Williams T, Moreen TR, Jazwinski A, Cruz B, Jeurkar N, Sapp R, Luo G, Liang TJ. 2005. An in vitro model of hepatitis C virion production. *Proc. Natl. Acad. Sci. U. S. A.* 102:2579–2583.
 60. Hijikata M, Shimizu YK, Kato H, Iwamoto A, Shih JW, Alter HJ, Purcell RH, Yoshikura H. 1993. Equilibrium centrifugation studies of hepatitis C virus: evidence for circulating immune complexes. *J. Virol.* 67:1953–1958.